Available online at www.sciencedirect.com
ScienceDirect
Dyes and Pigments 77 (2008) 7–15
DYES and PIGMENTS
www.elsevier.com/locate/dyepig

Selective heavy metal receptor functional phthalocyanines bearing thiophenes: Synthesis, characterization, spectroscopy and electrochemistry

Meryem N. Yarasir [a], Mehmet Kandaz [a,*], B. Filz Senkal [b], Atıf Koca [c], Bekir Salih [d]

[a] *Sakarya University, Department of Chemistry, 54140 Esentepe, Sakarya, Turkey*
[b] *Istanbul Technical University, Department of Chemistry, 34469 Maslak, Istanbul, Turkey*
[c] *Marmara University, Department of Chemical Engineering, Faculty of Engineering, 34722 Göztepe, Istanbul, Turkey*
[d] *Hacettepe University, Department of Chemistry, Faculty of Science, Beytepe Campus, 06532 Ankara, Turkey*

Received 12 December 2006; received in revised form 19 February 2007; accepted 21 February 2007
Available online 6 March 2007

Abstract

Soft metal ion receptor 2,9,16,23-tetrakis-6-(-thiophene-2-carboxylate)-hexylthio-phthlocyaninato zinc(II) and cobalt(II) complexes derived from 6-(3,4-dicyanophenylthio) hexylthiophene-2-carboxylate have been prepared as an isomeric mixture via cyclotetramerization reactions. The complexes have been fully characterized by elemental analysis, FTIR, ^{1}H and ^{13}C NMR, MS (ESI and MALDI-TOF) and by UV–vis spectral data. Soft metal ion binding ability of the complexes with Ag^{I}, Pd^{II}, Hg^{II} and Cd^{II} has been evaluated by UV–vis spectroscopic titration technique. Cyclic and differential pulse voltammetries show that while Zn(II)Pc gives up to two ligand-based reduction and one ligand-based oxidation processes having diffusion-controlled reversible electron transfer properties, Co(II)Pc represents one ligand-based and one metal-based oxidation and one metal-based and one ligand-based reduction processes having diffusion-controlled reversible electron transfer characters. Assignments of the redox couples of Co(II)Pc are confirmed by spectroelectrochemical measurements.

Keywords: Phthalocyanine; Zinc; Cobalt; Silver; Palladium; Ion receptor; MALDI-TOF; Electrochemistry; Spectroelectrochemistry

1. Introduction

In recent years, researcher's interest have focussed on phthalocyanines (Pc's) to perform specific functions such as semi-conductivity [1], chemical sensors [2,3], fibrous assemblies [4,5], photovoltaic [6], and optical data storage [7]. Incorporation of functionalities on the periphery of the phthalocyanines alters the technological applications by controlling the molecular assembly process of the phthalocyanine complexes [8,9]. Moreover, owing to their extended planar hydrophobic aromatic surface, phthalocyanine molecules can interact with each other by attractive π–π stacking interactions, leading aggregation both in solution and in the solid state [10–13]. Therefore, functional phthalocyanines are of particular chemical interest because of their tendency to aggregate in self-assemblies, optical and electrochemical responses to specific analyte, and capable of binding multiple metal ions for the development of new molecules/macrocycles [14–17]. For example, phthalocyanines bearing thia-oxo functionalities show optical changes when they bind Ag^{I} and Pd^{II} ions [18,19], while crown-attached phthalocyanines are well suited to bind alkaline and alkaline earth metal ions [14,15,20,21].

Thiol-derivatized metallophthalocyanine complexes show rich spectroscopic and photochemical properties. They are known to have absorption at longer wavelengths (>675 nm) than the other MPc complexes, a very useful feature for application in PDT, optoelectronics, fabrication of thin films such as the self-assembled monolayer (SAMs) and near-IR devices [2,4,5,11,22,23]. To date, a great variety of symmetrical or pseudo-symmetrical mononuclear phthalocyanines have been

* Corresponding author. Tel.: +90 264 295 59 46; fax: +90 264 295 59 50.
E-mail address: mkandaz@sakarya.edu.tr (M. Kandaz).

0143-7208/$ - see front matter © 2007 Elsevier Ltd. All rights reserved.
doi:10.1016/j.dyepig.2007.02.009

comprehensively studied. Nevertheless, there have been a limited number of reports on functional phthalocyanines, mainly because of the difficulties for preparation and purification [8,9,17,18,21,24]. Thus in this study as an extension of our previous research, we have prepared a new ionophore ligand, 6-(3,4-dicyanophenylthio)-hexylthiophene-2-carboxylate and its tetra-substituted metallophthalocyanines, {M[Pc($S-C_6H_{13}O COC_4H_3S)_4$]} (M = Zn, Co). Moreover, their electrochemical, spectroelectrochemical and specific cation binding properties have been investigated.

2. Experimental

Thiophene-2-carboxylic chloride, diethyl ether, tetrahydrofuran, dimethylsulfoxide, tetrabutylammonium perchlorate, $Zn(O_2CMe)_2$ and $CoCl_2$ were purchased from Aldrich, Merck and Alfa Aesar and used as received. Tetrahydrofuran was distilled from anhydrous $CaCl_2$ and acetophenone. 4-Nitro phthalonitrile and 4′-(6-hydroxyhexylthio)-1,2-dicyanobenzene were prepared according to literature [25,26]. Chromatography was performed with silica gel (Merck grade 60 and Sephadex) from Aldrich. The purity of the products was tested in each step by TLC (SiO_2, $CHCl_3$/MeOH, and THF/$CHCl_3$). All reactions were carried out under dry nitrogen atmosphere unless otherwise noted. ^{1}H NMR, and ^{13}C NMR spectra were recorded on a Bruker 300 spectrometer instrument. Multiplities are given as s (singlet), d (duplet), and t (triplet). FTIR (thin solution film) spectra were recorded on ATI Unicom-Mattson 1000 Spectrophotometer. Elemental analysis (C, H and N) was performed at the Instrumental Analysis Laboratory of Marmara University. Routine UV–vis spectra were obtained in a quartz cuvette on a Unicom UV-2 spectrometer.

2.1. Voltammetric measurements

The cyclic voltammetry (CV), differential pulse voltammetry (DPV), and controlled potential chronocoulometry (CPC) measurements were performed with a Princeton Applied Research Model VersaStat II potentiostat/galvanostat controlled by an external PC and utilizing a three-electrode configuration at 25 °C. The working electrode was a Pt plate with a surface area of 0.10 cm^2. The surface of the working electrode was polished with an H_2O suspension of Al_2O_3 before each run. The last polishing was done with a particle size of 50 nm. A Pt wire served as the counter electrode. Saturated calomel electrode (SCE) was employed as the reference electrode and separated from the bulk of the solution by a double bridge. Ferrocene was used as an internal reference. Electrochemical grade tetrabutylammonium perchlorate (TBAP) in extra pure dimethylsulfoxide (DMSO) was employed as the supporting electrolyte at a concentration of 0.10 mol dm^{-3}. High purity N_2 was used for deoxygenating the solution at least 15 min prior to each run and for maintaining a nitrogen blanket during the measurements.

For CPC studies, Pt gauze working electrode (10.5 cm^2 surface area), Pt wire counter electrode separated by a glass bridge, and SCE as a reference electrode were used. The spectroelectrochemical measurements were carried out using an Agilent model 8453 diode array spectrophotometer equipped with the potentiostat/galvanostat and utilizing a three-electrode configuration of thin-layer quartz spectroelectrochemical cell at 25 °C. The working electrode was transparent Pt gauze. Pt wire counter electrode and an SCE reference electrode, separated from the bulk of the solution by a double bridge were used.

2.2. MALDI mass spectrometry

Mass spectra were acquired on a Voyager-DE™ PRO MALDI-TOF mass spectrometer (Applied Biosystems, USA) equipped with a nitrogen UV-laser operating at 337 nm. Spectra were recorded both in linear and reflectron modes with an average of 50 and 100 shots for linear and reflectron modes.

2.3. MALDI sample preparation

2,5-Dihydroxy benzoic acid (DHB) for tetrakis-{6-(-thiophene-2-carboxylate)-hexylthio}-phthalocyaninato zinc(II) and 3-indole acrylic acid (IAA) (10 mg/mL in acetonitrile) for tetrakis-{6-(-thiophene-2-carboxylate)-hexylthio}phthalocyaninato cobalt(II) were prepared as MALDI matrix. MALDI samples were prepared by mixing the complexes (2 mg/mL in acetonitrile) with the matrix solution (1:10 v/v) in a 0.5 mL Eppendorf® microtube. Finally, 1 μL of this mixture was deposited on the sample plate, dried at room temperature and then analyzed.

2.4. Synthesis

2.4.1. 6-(3,4-Dicyanophenylthio)-hexylthiophene-2-carboxylate (*1*)

4′-Bis-(6-hydroxyhexylthio)-1,2-dicyanobenzene (0.5 g, 1.92 mmol) and triethylamine (0. 3 mL, 2. 1 mmol) were dissolved in THF (10 mL) at room temperature. The mixture was placed in an ice-bath. Then 2-thiophenecarbonyl chloride (0.25 cm^3 (excess)) was added dropwise into this mixture at 0 °C. The mixture was stirred for 1 h at 0 °C, then for 24 h at room temperature and finally heated for 2 h at 60 °C. After the reaction mixture was poured into water, the product was extracted with 50 cm^3 of diethyl ether. The organic extract was washed with water and dried over Na_2SO_4 and then, diethyl ether was removed by means of rotary evaporator. The final product was chromatographed over silica gel column using a mixture of $CHCl_3$/MeOH (100/2) as eluent, giving yellow 6-(3,4-dicyanophenylthio)-hexylthiophene-2-carboxylate (**1**). Finally pure powder was dried in vacua.

Yield: 0.65 g (87.2%), m.p.: 80 °C; FTIR (KBr thin film) ν/cm^{-1}: 2233 cm^{-1} (–CN), 3104, 3023 (Ar–H), 2929, 2888, 2859 (Aliph–CH_2) 1703 (–COOR, strong), 1581 (st), 1544, 1473,1390, 1286, 1191, 1128, 1072, 983, 873, 831, 719, 572; ^{1}H NMR (DMSO-d_6) δ: 7.88 (dd, 1H, *ortho* to COOR, thiophene H2), 7.80 (s, isomer, 1H, *meta* to CN and CS, Phenyl H5), 7.66 (dd, 1H, *ortho* to SR and CN, Phenyl H2), 7.70 (dd, 1H, *ortho* to CN, and Ar–H, thiophene H6), 7.63 (dd, 1H,

meta to Ar–S, and Ar–H, thiophene H5), 7.20 (dd, 1H, *meta* to thiophene–S, and thiophene–H, thiophene H4) 4.18 (t, br, $-CH_2$COOAliph (thiophene), 3.05 (CH_2CH_2–S–Ar), 1.63–1.78 (multiplet, 4H, $-O-CH_2CH_2-CH_2-$), 1.28–1.35 (multiplet, 4H, $-OCH_2CH_2CH_2-CH_2-$); ^{13}C NMR (300 MHz, δ, DMSO-d_6): 163.61, 162.16 (isomer), 147.46 (Bz), 134.31, 133.98, 133.90 (thiophene), 133.69, 131.00, 130.91 (Bz), 129.07, 128.92 (thiophene), 116.85, 116.37 (Bz), 115.78, 110.19, 65.38 (CH_2OCO), 40.44 (DMSO), 38.99 (S–CH_2), 30.99 (SCH_2CH_2), 28.58 (OCH_2CH_2), 28.29 (S$CH_2CH_2CH_2$), 25.64 ppm ($CH_2CH_2CH_2CH_2$O). Anal. Calc. for $C_{19}H_{18}N_2O_2S_2$ (370 g/mol) (%): C, 61.62; H, 4.86; N, 7.56; S, 17.30. Found (%): C, 61.13; H, 4.55; N, 7.28; S, 17.24. MS (ESI-MS) (%): *m/z* (%): 370 $[M+H]^+$ (27%).

2.4.2. 2,9,16,23-Tetrakis-{6-(-thiophene-2-carboxylate)-hexylthio}-phthalocyaninato zinc(II) (2)

A mixture of **1** (0.150 g, 0.405 mmol), anhydrous $Zn(O_2CMe)_2$ (0.019 g, 0.107 mmol), DBU (one drop) and quinoline ($\sim$1 cm^3) in a sealed tube was heated for 8 h with efficient stirring at 170–180 °C under N_2 atmosphere. After cooling to room temperature, the resulting solid was washed successively with MeOH, then cold MeCN, and finally *i*-PrOH and filtered to remove any inorganic and organic impurities until the filtrate was clear. The green-blue product (**2**) was isolated by silica gel column chromatography with $CHCl_3$ and then with THF/$CHCl_3$ (1:1 v/v) as eluent. Pure **2** was obtained as a viscous green oil after column chromatography over Sephadex (THF/$CHCl_3$, (1:1 v/v) as eluent) and then dried in vacua. This product is moderately soluble in $CHCl_3$ and shows excellent solubility in THF, DMF, DMSO and pyridine.

Yield: 0.036 g (23.0%). Anal. Calc. for $C_{76}H_{76}N_8O_8S_8Zn$ (1545 g/mol): C, 59.03; H, 4.92; N, 7.25; S, 16.57. Found: C, 58.74; H, 4.81; N, 7.01; S, 16.33; FTIR (KBr thin film) ν/cm^{-1}: 3091 (Ar–H), 2927, 2854 (Aliph–H), 1700 (COOR), 1600, 1522, 1448, 1417, 1356, 1310, 1256, 1224, 1142, 1087, 1070, 931, 897, 857, 816, 745, 718; ^{1}H NMR (DMSO-d_6) δ: 7.87 (dd, 1H, *ortho* to COOR, thiophene H2), 7.83 (s, isomer, 1H, *meta* to CN and CS, Phenyl H5), 7.67 (dd, 1H, *ortho* to SR and CN, Phenyl H2), 7.73 (dd, 1H, *ortho* to CN, and Ar–H, thiophene H6), 7.62 (dd, 1H, *meta* to Ar–S, and Ar–H, thiophene H5), 7.20 (dd, 1H, *meta* to thiophene–S, and thiophene–H, thiophene H4) 4.20 (t, br, $-CH_2$COO Aliph (thiophene), 3.02 (CH_2CH_2–S–Ar), 1.65–1.79 (multiplet, 4H, $-O-CH_2CH_2-CH_2-$), 1.27–1.34 (multiplet, 4H, $-OCH_2CH_2CH_2-CH_2-$); UV–vis (THF, λ_{max}/nm): 688, 660, 620, 355; MS (MALDI-TOF, 2,5-dihydroxy benzoic acid (DHB)) (10 mg/mL in MeCN as matrix): *m/z* (100%): 1546 $[M+H]^+$, and the peaks at 1547, 1548, 1549 and 1550 show the isotopic peak distributions of protonated molecular peak of the complex. $[M+K]^+$ observed at 1584.

2.4.3. 2,9,16,23-Tetrakis-{6-(-thiophene-2-carboxylate)-hexylthio}phthalocyaninato cobalt(II) (3)

Compound **1** (0.150 g, 0.405 mmol), DBU (one drop) and anhydrous $CoCl_2$ (left one night in oven at 110 °C) (0.013 g, 0.107 mmol) were pulverized and transferred to a tube and sealed under N_2 atmosphere and then it was immediately covered. The temperature of the reaction mixture was raised to 170–180 °C and kept for 12 h. After cooling to room temperature and diluting with *i*-PrOH, it was filtered. The dark green-blue crude product formed during the reaction was treated with *i*-PrOH several times and filtered off. It was then successively washed with H_2O and MeCN and then dried. Further purification by column chromatography with silica gel ($CHCl_3$/hexane as an eluent) was performed and dried in vacua. Solubility of the final product is moderate in $CHCl_3$, CH_2Cl_2 and excellent in THF, DMF, DMSO and quinoline.

Yield: 0.032 g (21.0%). Anal. Calc. for $C_{76}H_{76}N_8O_8S_8Co$ (1539 g/mol): C, 59.26; H, 4.94; N, 7.28; S, 16.62. Found: C, 58.89; H, 4.90; N, 7.03; S, 16.16; FTIR (KBr thin film) ν/cm^{-1}: 3091 cm^{-1} (Ar–H), 2928, 2854 (Aliph–H), 1701 (COOR, st), 1600, 1520, 1448, 1417, 1356, 1310, 1256 (st, Ar–S–CH_2), 1224, 1142, 1086 (st), 1071, 1038, 930, 897, 817, 748 (st), 717; UV–vis (THF, λ_{max}/nm): 676, 609, 401, 325; MS (MALDI-TOF, 3-indole acrylic acid (IAA) as matrix *m/z* (100%): 1539 $[M+H]^+$, and the peaks at 1540, 1541, 1542 and 1543 show the isotopic peak distributions of protonated molecular peak of the complex.

3. Results and discussion

Thiophene attached receptor metallophthalocyanines (**2** and **3**) in the present work were accomplished by heating pulverized mixture of **1** with either anhydrous $Zn(O_2CMe)_2$ or $CoCl_2$ salts at *ca*. 170–180 °C under nitrogen atmosphere in the presence of 1,8-diazabicyclo[5.4.0]undec-7-ene (DBU) as a strong base (Scheme 1). The yields of these reactions were rather low (23.0% for **2**, 21.0% for **3**). All final products were purified by numerous purifications via column chromatography over silica gel. Purification steps were tedious because of peripheral reactive end-group. The blue-green phthalocyanine products were isolated as an isomeric mixture as expected. The presence of isomers could be verified with slight broadening encountered in the UV–vis absorption bands and broadening in the ^{1}H NMR when compared with those of octa-substituted phthalocyanines composed of a single isomer [23]. The structure of **1** and each phthalocyanine was verified by FTIR, ^{1}H NMR, UV–vis and MALDI-TOF MS spectroscopic methods, as well as by elemental analysis. All the analytical and spectral data are consistent with the predicted structures.

While the major strong –CN band appeared at 2233 in the IR spectrum of **1** disappeared after conversion to metallophthalocyanines (**2** and **3**), the strong COOR band for **1** at around 1700 cm^{-1} came out with small shift. The aliphatic and aromatic peaks at above and below 3000 cm^{-1} and the rest of the spectra of **2** and **3** are closely similar to that of compound **1** and identified easily.

The ^{1}H NMR spectra of **2** was almost identical with the starting compound **1** except small shifts. The *ortho* aromatic protons to cyano group in the lower field region of the ^{1}H NMR and six different aromatic carbon atoms between 110

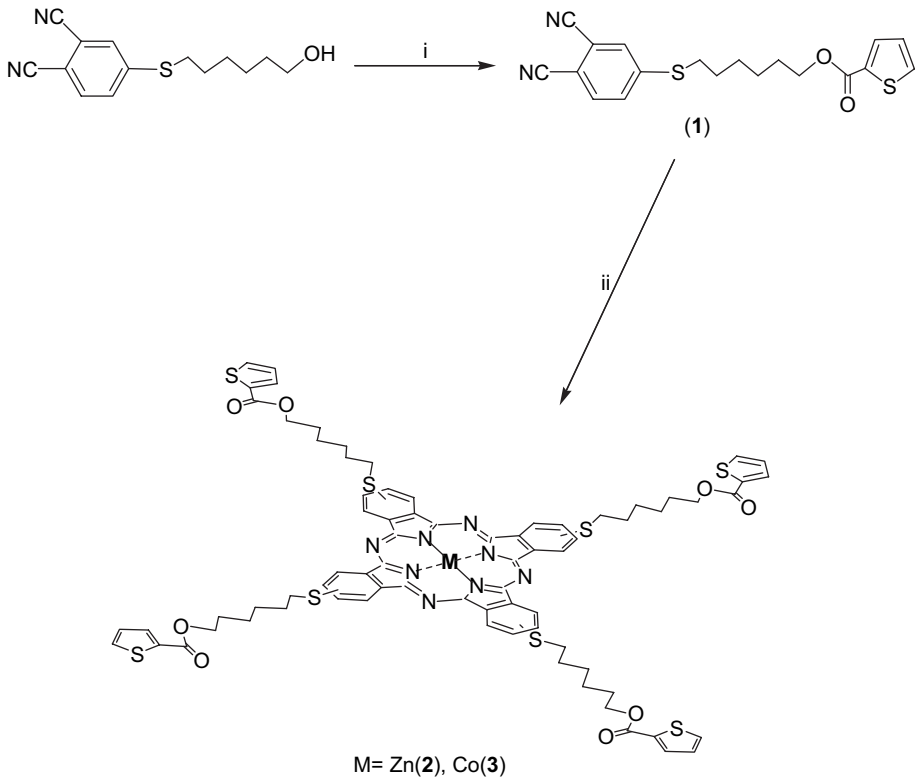

Scheme 1. Synthetic route of 2,9,16,23-tetrakis-{6-(-thiophene-2-carboxylate)-hexylthio}-metallophthalocyanine {M[Pc(S−$C_6H_{13}OH)_4$]$_2$} (M = Zn(II), Co(II)). (i) 2-Thiophenecarbonyl chloride, THF, −10 °C. (ii) Anhydrous Zn(acac)$_2$, $CoCl_2$, dbu.

and 145 ppm in ^{13}C APT spectrum are the instinctive indicator signals for **1** in addition to COOR signal at *ca*. 160 ppm. It is likely that the rather broad bands especially in the case of **2** were probably due to both chemical exchange associated with aggregation−disaggregation equilibrium and is a mixture of four positional isomers. Aggregation−disaggregation equilibrium occurred at high concentrations used in the NMR measurements. The product obtained in these reactions is a mixture of four positional isomers that are expected to show chemical shifts only slightly differing from each other [23,26].

UV−vis spectra of the phthalocyanine complexes exhibit characteristic Q- and B-bands. The Q-band in the visible region at *ca*. 600−750 nm (Q-band) is attributed to the π−π* transition from HOMO (highest occupied molecular orbital) to the LUMO (lowest unoccupied molecular orbital) of the Pc(−2) ring, and the B-band in the UV region at *ca*. 300−400 nm (B-band) arises from the deeper π−π* transitions [27]. The absorption positions of the synthesized compounds are dependent on the ionic radius of the metal center. The wavelength of the absorption shifts to the red region as the radius of the metal center increases. The Q-band absorptions in the UV−vis absorption spectra of **2** and **3** were observed as a single band with a high intensity due to a single π−π* transition at 688 and 675 nm, respectively, with shoulders at slightly higher energy side of the Q-band for each phthalocyanine. The effect of *S*-substitution on the periphery for the phthalocyanines was a shift in the Q-bands to longer wavelengths because of the electron-donating thioether substituents when compared with those of unsubstituted and alkyl or *O*-substituted derivatives [14,15,17−19]. The extent of aggregation affected by *S*-substitution on the periphery was slightly stronger for the phthalocyanines bearing tetra-substituents on the periphery than that for the octa-substituted ones [11,12,28].

3.1. MALDI-TOF mass spectra

MALDI-MS spectroscopy has been extensively used to characterize metal-based phthalocyaninates. Therefore, the mass spectra of **2** and **3** confirmed the proposed structures. MALDI-MS spectra of **2** and **3** are given in Figs. 1 and 2. The protonated mono isotopic molecular ion peaks were easily identified at *m*/*z*: 1546 $[M + H]^+$ for **2** and *m*/*z*: 1539 $[M + H]^+$ for **3**.

Protonated molecular ion peak was observed at 1546 Da that was exactly overlapped with the mass of the lowest mass of the isotopic mass distribution of complex **2** calculated theoretically from the elemental composition of the zinc complex. Isotopic peaks resulted from isotopic distribution of the protonated molecular ion of **2** were observed in between 1544 and 1553 Da with 1 Da increment in the high mass range (Fig. 1). Following the protonated molecular ion peak, a peak group was observed at 38 Da mass higher than the protonated molecular ion peak group resulting in almost same pattern. This peak resulted from the potassium adduct to the neutral molecule of **2**. Beyond the protonated molecular ion, potassium adduct and one fragment peaks of **2** at 1463 *m*/*z* representing thiophene side chain leaving group, the MALDI mass spectrum of **2** showed a very clear spectrum.

Positive ion MALDI-MS spectrum of complex **3** is given in Fig. 2. Many different MALDI matrixes were tried to find

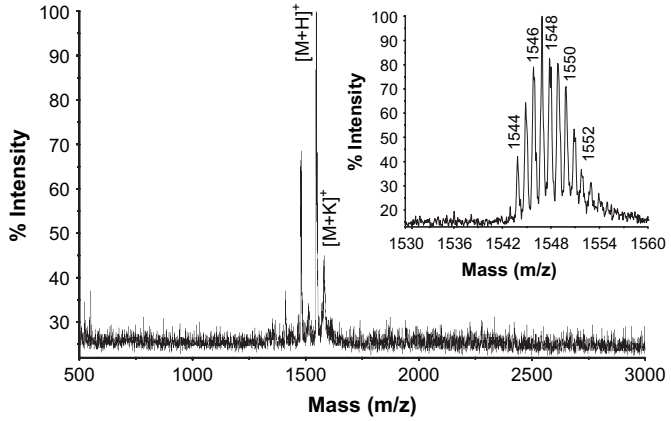

Fig. 1. Positive ion and reflectron mode MALDI-MS spectrum of **2** obtained in 3-indole acrylic acid MALDI matrix using nitrogen laser accumulating 50 laser shots. Inset spectrum shows expanded molecular mass region of the complex.

intense molecular ion peak and low fragmentation under the MALDI-MS conditions for this complex. The peak group representing the protonated molecular ion of **3** was observed starting with 1539 Da mass and finishing 1544 Da following each other by 1 Da mass differences. This type of mass distribution resulted from the isotopic mass distribution of carbon (mainly ^{13}C) and the isotopes of cobalt in the metal complex of ligand. In the MALDI-MS spectrum of **3**, besides the protonated molecular ion peak, some intense fragment ions resulting from side chain thiophene leaving groups and sodium adducts were observed. This pointed out the fact that no intense leaving groups were available from this complex and the complex was very stable under the MALDI matrix conditions and under the laser energy.

3.2. Spectroscopic metal ion binding titrations

Sulphur donor atoms on the periphery of phthalocyanines act as heavy metal ionophore and impart a preference for coordination with soft heavy metal ions with different size, such as Ag^I, Cu^I and Pd^{II} [17–20,29]. To analyze the metal ion

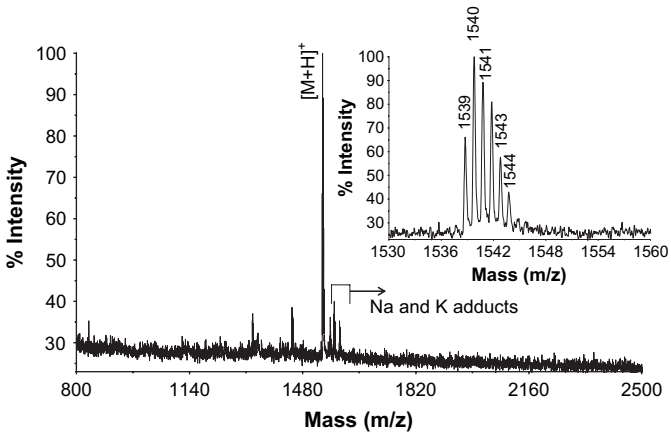

Fig. 2. Positive ion and reflectron mode MALDI-MS spectrum of **3** obtained in 3-indole acrylic acid MALDI matrix using nitrogen laser accumulating 50 laser shots. Inset spectrum shows expanded molecular mass region of the complex.

binding ability of **2** and **3**, peripheral soft-acid soft-base coordination is monitored by UV–vis spectroscopic titration with Ag^I, Cd^{II} and Pd^{II}. Titration experiments were carried out using THF/MeOH (5:1, v/v) solution of **2** and **3** to ensure complete dissolution of the analyte salts, $AgNO_3$, Na_2PdCl_4, $HgCl_2$ and $CdCl_2$ dissolved in MeOH. Here the concentration of each MPc and the metal salt was *ca.* 10^{-4} and 10^{-2} mol dm^{-3}, respectively. The reason for the higher concentration of the metal salt was to produce negligible changes by dilution after its addition to phthalocyanine solution. Blank tests were performed to evaluate the effect of the dilution.

The room temperature gradual addition (μL) of Ag^I and Pd^{II} to the THF/MeOH solution of **2** and **3** caused a gradual color change, from blue-green to intractable black-dark green in the case of Ag^I, to less soluble dark green in the case of Pd^{II}, suggesting the complex formation of **2** and **3** with Ag^I and Pd^{II}. During the titration, an intractable precipitate that could not be isolated formed. Fig. 3 (A and B) shows that Ag^I binding to the donor atoms of **2** and **3** results in pronounced effects in the Q- and B-bands (blue shift), and in the n–π* transitions. As shown in Fig. 3, gradual addition of small increments of Ag^I to **2** and **3** leads to gradual disappearance of the Q-bands at 688 and 675 nm assigned to the monomeric species, and simultaneous enhancement of the intensity of the oligomeric aggregated species around 645 and 627 nm, respectively. The B-bands of the complexes shift to higher energy sides about 5–20 nm, such as from 357 to 350 nm for **2** and from 330 to 314 nm for **3** with small changes in intensity. These spectroscopic changes indicate the coordination of Ag^I by the donor atoms of the phthalocyanines to form less soluble oligomeric aggregated species. As appeared in Fig. 3 (A and B), the titrations show clear isosbestic points at 326, 372, 403, 470, 607, 624, 669 and 710 nm for **2** and 362, 420, 642 and 709 nm for **3**. This observation is in harmony with the previously reported studies [15,18,19,29,30].

On the other hand, the titration of **2** and **3** with Pd^{II} gives somewhat different spectra (Fig. 3C). Addition of Pd^{II} in MeOH to the solutions of **2** and **3** in THF/MeOH (5:1, v/v) causes an immediate color change, from blue-green to green, suggesting complex formation. This color change was followed by the formation of less intractable green solid, which precluded its purification [29]. This type of spectroscopic behavior probably results from the effect of Pd^{II} on the aggregation–disaggregation equilibrium and suggesting square-planar formation. This means that the complexation of the complexes with Pd^{II} decreases the concentration of monomeric units in some degree but do not increase dimeric units by intramolecular sandwich formation. Consequently, the interaction of Pd^{II} ion with the peripheral moieties of the complexes causes to decomposition of the aggregates of planar phthalocyanine molecules in solution [30].

Borderline-metals, such as Hg^{II} and Cd^{II} did not show significant change in the UV–vis spectrum of **2** and **3** upon addition of $HgCl_2$ and $CdCl_2$ except for the small decrease in intensity due to dilution. The lack of change in the UV–vis spectrum would be consistent with very weak or no coordination of the S atoms on the periphery to the mercury or cadmium ion [29].

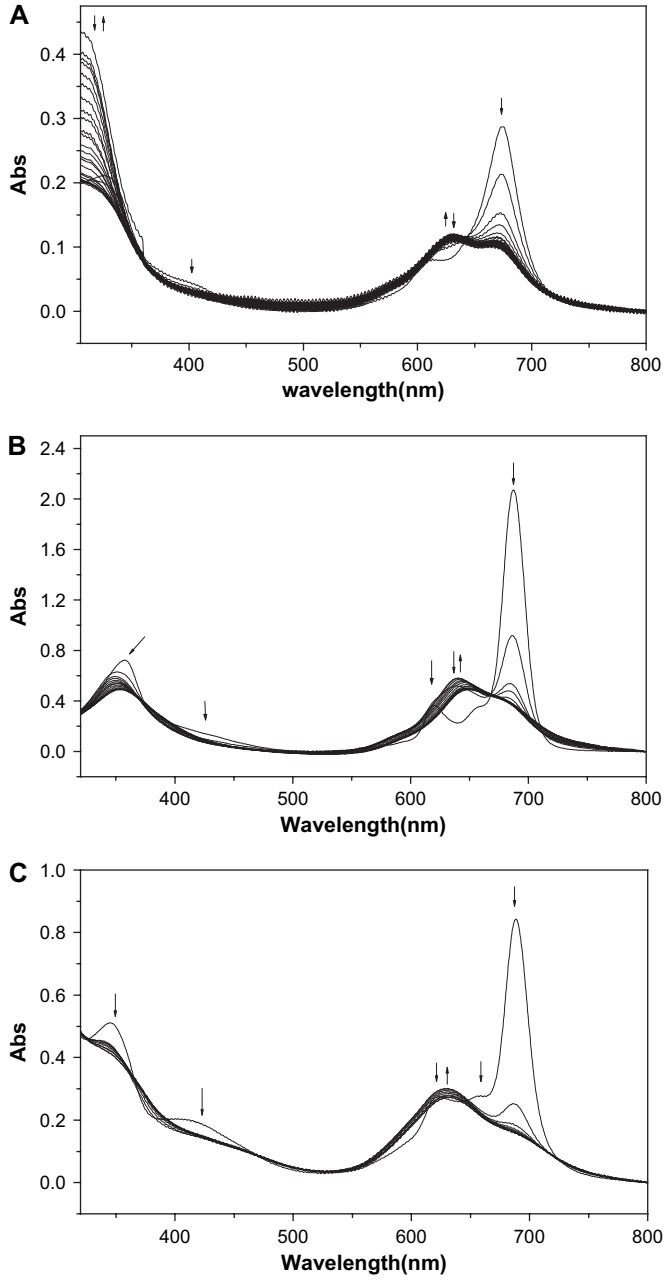

Fig. 3. UV–vis spectra of **2** (A) and **3** (B) in THF/MeOH during titration by Ag^{I} (in MeOH). (C) Titration of **3** by Pd^{II} in MeOH.

3.3. Electrochemical measurements

The electrochemical behavior of the phthalocyanines was investigated by cyclic voltammetry (CV) and differential pulse voltammetry (DPV) on a platinum working electrode in DMSO. The half-wave redox potential values ($E_{1/2}$) vs. SCE, anodic to cathodic peak separation (ΔE_p) and peak current ratios (I_{pa}/I_{pc}) are summarized in Table 1.

The CV and DPV of **2** are represented in Fig. 4. While complex **2** gives an oxidation couple at 0.67 V during the anodic scan, upon cathodic potential sweep, three cathodic waves are recorded (R_1 at −0.73 V, R_2 at −1.13 V and R'_2 at −1.43 V at 100 mV s^{-1} scan rate). For couples R_1 and R_2, the anodic to cathodic peak currents (I_{pa}/I_{pc}) were near unity and anodic to cathodic peak separation (ΔE_p) ranged from 70 to 130 mV with increasing scan rates, thus suggesting reversible to quasi-reversible behavior (ΔE_p's, 60–110 mV, were obtained for ferrocene standard). DPV of the complex confirms the recorded redox processes and the reversibility of the electron transfer processes clearly (insets in Fig. 4). When we analyze the reduction processes, it is clearly shown that the peak current of R_1 is twofold that of the R_2 and R'_2. The peak separation (0.40 V) and position of R_1 and R_2 are concurred with the first and second reduction of the MPc's. However, R'_2 is very close to R_2, so it could not be the third reduction process, since the peak separation of the second and third reduction couples are approximately between 0.80 and 1.00 V for MPc's. These voltammetric data indicate that these uncommon behaviors may be resulted from the aggregation of the complex. Thus R_1 couple could be assigned to the reduction of the aggregated species while the R_2 and R'_2 processes show the aggregation–disaggregation equilibrium as shown in Eq. (1). The peak current of R_1 decreased and the peak current of R_2 increased while the peak current of R_2' decreased with dilution of the solution. This effect supports the aggregation of the complex in solution.

$$
\begin{array}{l}
[\,\mathrm{Zn(II)Pc(-1)}]^{+} \\
\quad e^{-} \Updownarrow 0.67\mathrm{V} \\
[\,\mathrm{Zn(II)Pc(-2)}]_{\mathrm{Agg.}} \underset{-0.73\mathrm{V(R_1)}}{\overset{e^{-}}{\Leftrightarrow}} [\,\mathrm{Zn(II)Pc(-3)}]^{-}{}_{\mathrm{Agg.}} \Leftrightarrow [\,\mathrm{Zn(II)Pc(-3)}]^{-}{}_{\mathrm{Disagg.}} \\
\qquad\qquad \underbrace{e^{-} \Updownarrow -1.43\mathrm{V(R'_2)} \qquad e^{-} \Updownarrow -1.13\mathrm{V(R_2)}}_{[\,\mathrm{Zn(II)Pc(-4)}]^{2-}}
\end{array}
\tag{1}
$$

Table 1
Voltammetric data for the complexes **2** and **3**

Complexes	O_2	O_1			R_1			R_2			R_3
	$E_{1/2}$[a] (V)	$E_{1/2}$[a] (V)	ΔE_p[b] (mV)	I_{pc}/I_{pa}[c]	$E_{1/2}$[a] (V)	ΔE_p[b] (mV)	I_{pc}/I_{pa}[c]	$E_{1/2}$[a] (V)	ΔE_p[b] (mV)	I_{pc}/I_{pa}[c]	$E_{1/2}$[a] (V)
2		0.67	116	0.90	−0.73	71	1.00	−1.13	60	0.78	−1.43[e]
3	0.99[d]	0.49	88	1.01	−0.36	70	0.98	−1.27	74	0.75	−1.83[d]

[a] $E_{1/2} = (E_{pa} + E_{pc})/2$ at 100 mV s^{-1}.
[b] $\Delta E_p = E_{pa} + E_{pc}$ at 100 mV s^{-1}.
[c] I_{pa}/I_{pc} for reduction, I_{pc}/I_{pa} for oxidation processes at 100 mV s^{-1}.
[d] Determined by DPV.
[e] R'_2 wave of the complex.

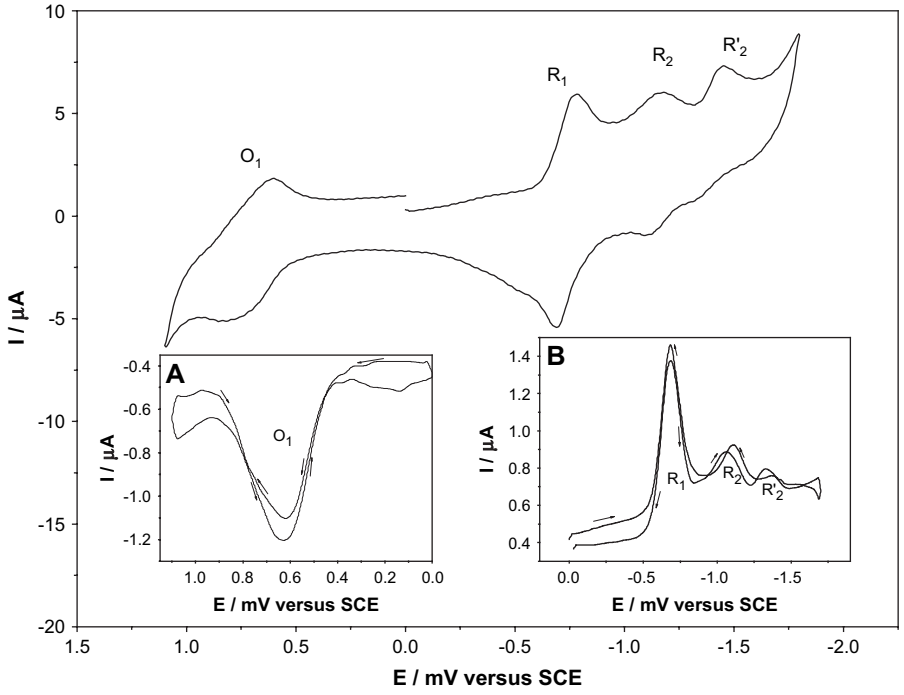

Fig. 4. Cyclic and differential pulse voltammograms of **2** (A = oxidation) (B = Reduction) at 100 mV s^{-1} scan rate on Pt in DMSO/TBAP.

Fig. 5 shows the CV and DPV of complex **3**. Within the electrochemical window of TBAP/DMSO, **3** undergoes one quasi-reversible one-electron oxidation process labeled as O_1 at 0.49 V and two reversible one-electron reductions labeled as R_1 and R_2, at −0.360, and −1.27 V vs. SCE at 0.100 V s^{-1} scan rate. Moreover, at the end of the solvent window, a reversible oxidation couple at 0.99 V and a quasi-reversible reduction couple at −1.83 V are recorded by DPV. First-row transition metal Pc's differ from those of the main-group metal Pc's because metal "d" orbitals may be positioned between HOMO and LUMO of the

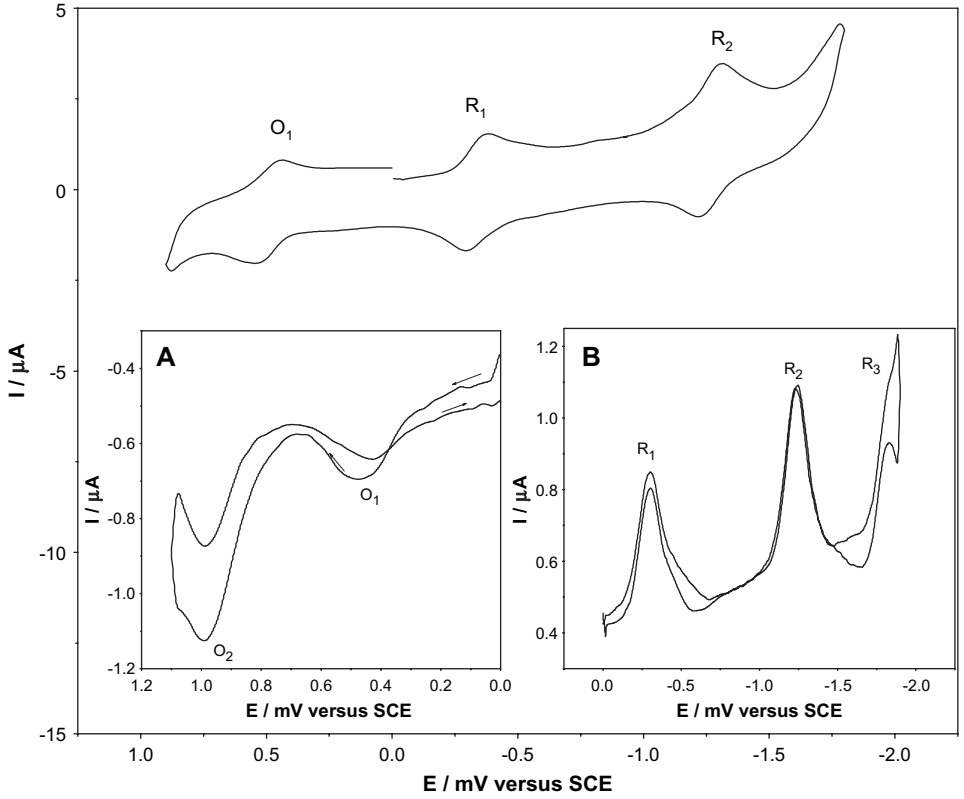

Fig. 5. Cyclic and differential pulse voltammograms of **3** (A = oxidation) (B = reduction) at 100 mV s^{-1} scan rate on Pt in DMSO/TBAP.

phthalocyanine (Pc(−2)) ligand. The first oxidation and first reduction processes occur on the metal center in the metal Pc only for Mn, Fe and Co derivatives in polar solvent such as DMF and DMSO. For Ni, Cu and Zn phthalocyanines, redox processes take place on the Pc ring [1,8,31–37]. This study indicates that the first reduction and first oxidation processes of **3** recorded at 0.49 and −0.36 could be assigned easily to the Co^{II}/Co^{III} and Co^{II}/Co^{I} redox couple, respectively, and the remaining processes to the phthalocyanine ring. All predicted redox processes are given in Eq. (2). Furthermore, both the first oxidation and the first reduction of **3** are recorded almost at the same potentials relative to those of reported for CoPc (Table 1). The separation between the metal center reduction and oxidation processes (∼0.85 V) is comparable with the CoPc papers [1,8,31–37].

$$
\begin{array}{ccccc}
[\,\mathrm{Co\,(III)\,Pc\,(-2)}]^{+} & \underset{0.99\ \mathrm{V}}{\overset{e^-}{\Leftrightarrow}} & [\,\mathrm{Co\,(III)\,Pc\,(-1)}]^{2+} & & \\
e^- \Updownarrow 0.49\ \mathrm{V} & & & & \\
[\,\mathrm{Co\,(II)\,Pc\,(-2)}] & \underset{-0.36\ \mathrm{V}}{\overset{e^-}{\Leftrightarrow}} & [\,\mathrm{Co\,(I)\,Pc\,(-2)}]^{-} & \underset{-1.27\ \mathrm{V}}{\overset{e^-}{\Leftrightarrow}} & [\,\mathrm{Co\,(I)\,Pc\,(-3)}]^{2-} \\
 & & & \underset{-1.83\ \mathrm{V}}{\overset{e^-}{\Leftrightarrow}} & [\,\mathrm{Co\,(I)\,Pc\ (-4)}]^{3-}
\end{array}
\qquad (2)
$$

For the couples, anodic to cathodic peak separations (ΔE_p) changing from 60 to 120 mV with the scan rates from 10 to 500 mV s^{-1} (ΔE_p's, 60–110 mV, were obtained for ferrocene reference) support reversible electron transfer. Reversibility is illustrated by the similarity in the forward and reverse DPV scans (insets in Fig. 5) [19,34]. The values of I_{pa}/I_{pc} for all couples of complex **3** are close to unity and the peak currents increased linearly with the square root of scan rates, for scan rates ranging from 10 to 500 mV s^{-1}, indicating that the electrode reactions are purely diffusion-controlled for the couples.

3.4. Spectroelectrochemical studies

Complex **2** has electro-inactive metal center and so all redox couples are undoubtedly assigned to phthalocyanine ring. To confirm the assignment for **3**, spectroelectrochemical measurements were carried out. Fig. 6A illustrates the UV–vis spectra of the neutral and electrogenerated species of **3** after the applied potentials to each redox process. Fig. 6B shows the UV–vis spectral changes during a controlled potential reduction of **3** at −0.50 V vs. SCE corresponding to the redox process labeled R_1 in the CV (Fig. 5). The Q-band at 675 nm decreases in

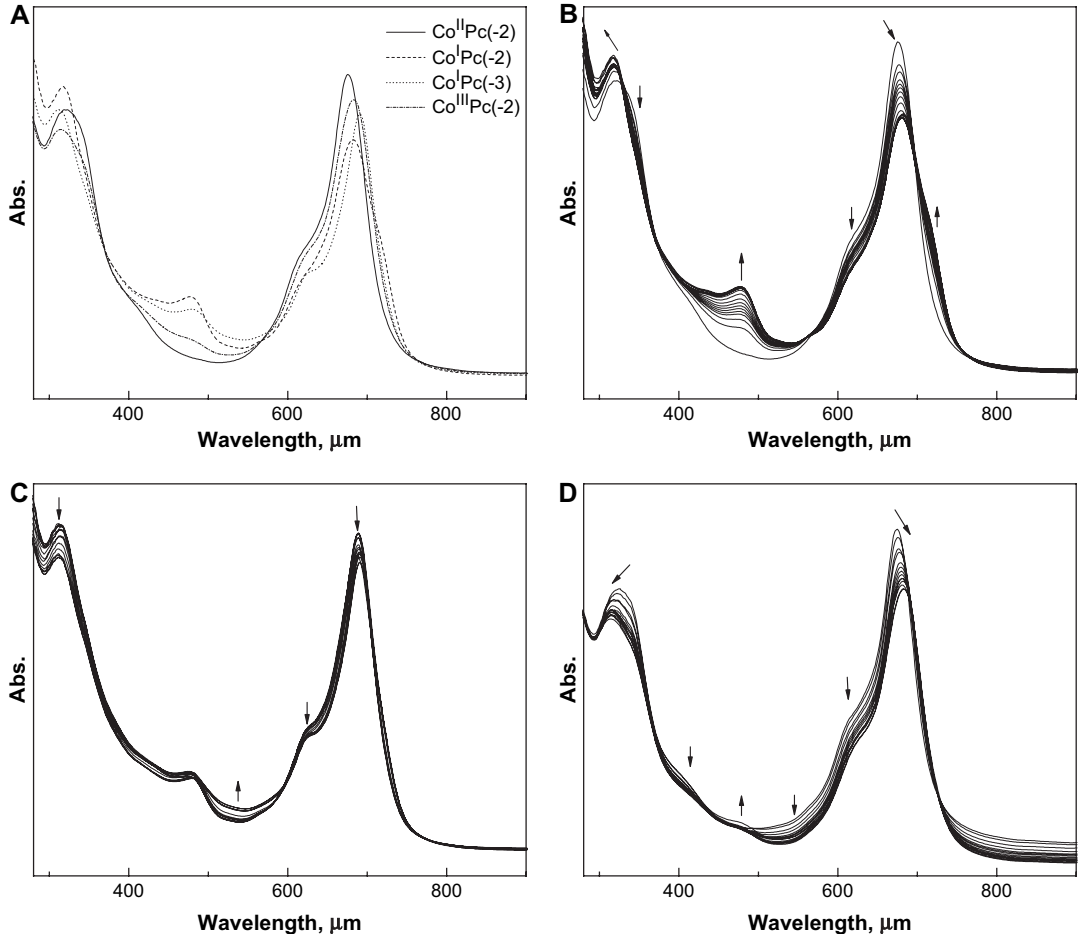

Fig. 6. UV–vis spectra of **3**. (A) UV–vis spectra of the neutral and electrogenerated species of **3** at the end of the each redox potential. (B) In situ UV–vis spectral changes of **3** at −0.50 V corresponding to the redox process labeled R_1. (C) In situ UV–vis spectral changes of **3** at −1.30 V corresponding to the redox process labeled R_2. (D) In situ UV–vis spectral changes of **3** at 0.55 V corresponding to the redox process labeled O_1.

intensity with a red shift to 683 nm while two new bands at 720 and 480 nm appear as the reduction process continues. The shoulder of B-band at 344 nm decreases while the intensity of B-band at 322 nm increases with blue shift to 316 nm during the process. The band at 480 nm and decrease of Q-band with blue shift indicate the formation of the $[Co(I)Pc(-2)]^{1-}$ species, confirming the CV assignment of couple R_1 to $[Co(II)Pc(-2)]/[Co(I)Pc(-2)]^{1-}$ couple [1,38–43]. This process resulted with clear isobestic points at 328, 370, 335, 562, 696 and 766 nm in the spectra. The spectral changes in Fig. 6C are typical of ring-based reduction in phthalocyanine complexes [1,38–43]. There was no change in the intensity of the band at 480 nm and an increase in the intensity of Q-band without shift upon further reduction of the $[Co(I)Pc(-2)]^{1-}$ species at the potential of couple R_2. The intensity of B-band decreases without shift during this process. This process resulted with clear isobestic points at 490, 598, 707 and 778 nm in the spectra. This confirms our earlier assignment of the process labeled R_2 to $[Co(I)Pc(-2)]^{1-}/[Co(I)Pc(-3)]^{2-}$. Fig. 6D shows the spectral changes observed when the potential corresponding to process O_1 was applied to the solution of $[Co^{II}Pc\ (-2)]$. The Q-band at 675 nm decreases in intensity with red shift to 685 nm while new bands at 480 nm appear as the oxidation process continues. The B-band at 322 nm decreases with blue shift to 313 nm while the intensity of the band at 405 nm decreases during the process. The band at 480 nm and decrease of Q-band with red shift are typical of a metal-based oxidation in cobalt Pc complexes. The final spectrum in Fig. 6D is therefore assigned to $[Co(III)Pc(-2)]^{1+}$, confirming CV assignments. This process resulted with clear isobestic points at 365, 437, 485, 690 and 730 nm in the spectra.

Acknowledgements

We thank the Research Funds of Sakarya University (project no: 2002-45), DPT-2004 (project no: 2003K120970).

References

[1] Leznoff CC, Lever ABP. In: Leznoff CC, Lever ABP, editors. Phthalocyanines: properties and applications, vols. 1–4. Weinheim: VCH; 1989–1996.
[2] Sadaoka Y, Jones TA, Göpel W. Sens Actuators B 1990;1:148.
[3] Simon JJ, Andre HJ. Molecular semiconductors. Berlin: Springer; 1985.
[4] Takahashi R, Kobuke Y. J Am Chem Soc 2003;125:2372.
[5] Chen X, Drain CM. Encycl Nanosci Nanotechol 2004;9:593.
[6] Raid AS, Korayem MT, Abdel-Malik TG. Physica B 1999;270:140.
[7] Ao R, Kilmmert L, Haarer D. Adv Mater 1995;7:495.
[8] Kobayashi N, Sasaki N, Higashi Y, Osa T. Inorg Chem 1995;34:1636.
[9] Zhong C, Zhao M, Stern C, Barrett AGM, Hoffman BM. Inorg Chem 2005;44:8272.
[10] Li X, He X, Ng ACH, Ng DKP, Wu C. Macromolecules 2000;33:2119.
[11] Cook MJ. J Mater Chem 1996;6:677.
[12] Hanack M, Lang M. Adv Mater 1994;6:819.
[13] Tau P, Nyokong T. Polyhedron 2006;25:1802.
[14] Kandaz M, Yılmaz I, Bekaroğlu Ö. Polyhedron 2000;19:115.
[15] Kandaz M, Bekaroğlu Ö. J Porphyrins Phthalocyanines 1999;3:339.
[16] Zhao Z, Ozoemena KI, Maree DM, Nyokong T. J Chem Soc Dalton Trans 2005;1241.
[17] Goldberg DP, Michel Sarah LJ, White AJP, Williams DJ, Barrett AGM, Hoffman BM. Inorg Chem 1998;37:2100.
[18] Michel SLJ, Barrett AGM, Hoffman BM. Inorg Chem 2003;42:814.
[19] Kandaz M, Çetin HS, Koca A, Özkaya AR. Dyes Pigments 2007;74:298.
[20] Koray AR, Ahsen V, Bekaroğlu Ö. J Chem Soc Chem Commun 1986;932.
[21] Michel SLJ, Goldberg DP, Stern C, Barrett AGM, Hoffman BM. J Am Chem Soc 2001;123:4741.
[22] Rosential I. In: Leznoff, Lever ABP, editors. The phthalocyanines properties and applications, vol. 4. New York: VCH; 1996. p. 485–514.
[23] Kandaz M, Michel SLJ, Hoffman BM. J Porphyrins Phthalocyanines 2003;7:700.
[24] Muranaka A, Yoshida K, Shoji T, Moriichi N, Masumoto S, Kanda T, et al. Org Lett 2006;8(12):2447.
[25] Snow AW, Griffith JR. Macromolecules 1984;17:1614.
[26] Yarasir MN, Kandaz M, Koca A, Salih B. Polyhedron 2007;26:1139.
[27] Gouterman M. In: Dolphin D, editor. The porphyrins, vol. 3. New York: Academic Press; 1978. p. 1–65.
[28] Kandaz M, Bekaroğlu Ö. Chem Ber 1997;135:1833.
[29] Lange SJ, Sibert JW, Barrett AGM, Hoffman BM. Tetrahedron 2000;56:7371.
[30] Gürol İ, Ahsen V, Bekaroğlu Ö. J Chem Soc Dalton Trans 1994;497.
[31] Mc Keown NB. Phthalocyanines materials: synthesis, structure and function. New York: Cambridge University Press; 1998.
[32] Kobayashi N, Ogata H, Nonaka N, Luk'yanets EA. Chem Eur J 2003;9:5123.
[33] Abdurrahmanoğlu Ş, Özkaya AR, Bulut M, Bekaroğlu Ö. Dalton Trans 2004;4022.
[34] Kandaz M, Yaraşır MMU, Koca A, Bekaroğlu Ö. Polyhedron 2002;21:255.
[35] Kalkan A, Koca A, Bayır ZA. Polyhedron 2004;23:3155.
[36] Koca A, Şener MK, Koçak MB, Gül A. Transition Met Chem 2005;30(4):399.
[37] Koca A, Dinçer HA, Koçak MB, Gül A. Russ J Electrochem 2006;41(1):36.
[38] Obirai J, Nyokong T. Electrochim Acta 2005;50:5427.
[39] Sehlotho N, Nyokong T. Electrochim Acta 2005;51:4463.
[40] Koca A, Dinçer HA, Çerlek H, Gül A, Koçak MB. Electrochim Acta 2007;52:2683.
[41] Hesse K, Schlettwein D. J Electroanal Chem 1999;476:148.
[42] Jin Z, Nolan K, McArthur CR, Lever ABP, Leznoff CC. J Organomet Chem 1994;468:205.
[43] Tse YH, Goel A, Hu M, Leznoff CC, Van Lier JE, Lever ABP. Can J Chem 1993;71:742.